

Tripodal structure in undersaturated random graphs

William DiCarlo and Lorenzo Sadun*

ABSTRACT

We numerically investigate typical graphs in a region of the Strauss model of random graphs with constraints on the densities of edges and triangles. This region, where typical graphs had been expected to be bipodal but turned out to be tripodal, involves edge densities e below $e_0 = (3 - \sqrt{3})/6 \approx 0.2113$ and triangle densities t slightly below e^3 . We determine the extent of this region in (e, t) space and show that there is a discontinuous phase transition at the boundary between this region and a bipodal phase. We further show that there is at least one phase transition within this region, where the parameters describing typical graphs change discontinuously.

Keywords: graphon, entropy, Erdős-Rényi, phase transition, tripodal

2020 Mathematics Subject Classification: 05C80, 60C05, also 05C35, 82-05.

1. Introduction and results

1.1. Background

We are investigating the structure of large random graphs with specified densities (e, t) of edges and triangles, the so-called Strauss model [20]. More precisely, we consider the ensemble of all graphs on n vertices that have the specified densities of edges and triangles, up to a small tolerance that goes to zero as $n \rightarrow \infty$. For most values of (e, t) , there is a typical structure to such graphs, with all but a tiny fraction having essentially the same statistical properties. The fundamental question is understanding how this structure varies with (e, t) . In this paper we study this question when t is slightly below e^3 and e is less than the threshold $e_0 = (3 - \sqrt{3})/6 \approx 0.2113$.

The key algebraic tool is *graphons* (see [10] for an overview of this expansive subject and [2, 3, 11] for some original references). A graphon is a measurable function $g :$

* Corresponding author.

$[0, 1]^2 \rightarrow [0, 1]$ with $g(x, y) = g(y, x)$. This can be viewed either as a limit of large graphs or as a random process for producing graphs. To generate a graph on n vertices from a graphon, first pick n numbers x_i independently and uniformly on $[0, 1]$. Then flip $\binom{n}{2}$ independent biased coins, assigning an edge to vertices i and j with probability $g(x_i, x_j)$. The statistical properties of graphs that are generated this way are easy to read off from the graphon. For instance, the expected densities of edges and triangles are

$$\varepsilon(g) := \int_0^1 \int_0^1 g(x, y) dx dy \quad \text{and,} \quad (1)$$

$$\tau(g) := \int_0^1 \int_0^1 \int_0^1 g(x, y)g(y, z)g(z, x) dx dy dz, \quad (2)$$

respectively. As $n \rightarrow \infty$, the variance in the edge and triangle densities go to zero, so almost all graphs generated by g have edge and triangle densities close to $(\varepsilon(g), \tau(g))$. We can thus speak of $\varepsilon(g)$ and $\tau(g)$ as the edge/triangle densities of the graphon, and not just as the *expected* densities.

The number of graphs that are created in this way is determined by the Shannon entropy of the graphon,

$$S(g) := \int_0^1 \int_0^1 H(g(x, y)) dx dy, \quad (3)$$

where

$$H(u) = -(u \ln(u) + (1 - u) \ln(1 - u)),$$

is the usual entropy of a coin flip with probability u of getting heads. Thanks to the large deviations principle of Chatterjee and Varadhan [4] and to subsequent work by Radin and Sadun [16], understanding the typical structure of graphs with edge/triangle densities (e, t) is equivalent to finding the graphon g that maximizes $S(g)$ subject to the constraints $(\varepsilon(g), \tau(g)) = (e, t)$. If $\tilde{g}(x, y) = g(\sigma(x), \sigma(y))$, where σ is a measure-preserving transformation of $[0, 1]$, then \tilde{g} and g have the same densities and the same entropy. Indeed, they generate the same graphs on n vertices with exactly the same probabilities! When we apply constraints, maximize the entropy, and speak of the optimal graphon being unique, we always mean “unique up to measure-preserving transformation.” (In general one must mod out by the closure of this equivalence relation with respect to a certain “cut norm”. However, the relation applied to the “multipodal” graphons considered in this paper is already closed, so we can ignore that complication.)

If the entropy-maximizing graphon g with edge/triangle densities (e, t) is unique (up to measure-preserving transformations), then the ensemble of large graphs with edge/triangle densities close to (e, t) is essentially the same as the ensemble of large graphs generated by g . Specifically, for any $\epsilon > 0$ there exists a constant $K > 0$ such that all but a fraction e^{-Kn^2} of the graphs on n vertices with edge/triangle densities close to (e, t) are within ϵ of g in the “cut metric” [16, 17]. Conversely, all but an exponentially small fraction of the graphs generated by g have edge/triangle densities close to (e, t) . The combinatorial problem of understanding typical graphs with specified edge/triangle densities thus reduces to the analytic problem of maximizing $S(g)$ subject to the constraints $(\varepsilon(g), \tau(g)) = (e, t)$.

The space of all possible values of (e, t) in the edge-triangle model was first worked out by Razborov [19] (see also [15]) and is called the Razborov triangle, see Figure 1. A *phase* is an open subset of the Razborov triangle where the typical structure is a real-analytic function of (e, t) in the sense that the optimal graphon is unique and depends analytically on (e, t) . This implies that the density of any fixed subgraph, such as a square or pentagon or tetrahedron, is also an analytic function of (e, t) . At a phase boundary, the optimal graphon fails to be analytic and may even change discontinuously, implying an abrupt change in the density of some subgraph.

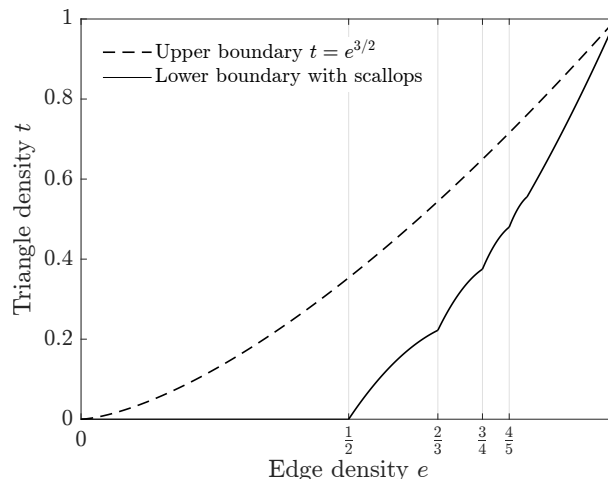


Fig. 1. The Razborov triangle. The curvature of the “scallops” on the lower right is exaggerated for visibility

In 2017, [8] conjectured that the Razborov triangle consisted of one phase above the “Erdős-Rényi” curve $t = e^3$ and three infinite families of phases below the Erdős-Rényi curve, see Figure 2 for a schematic phase diagram. The conjectured phase picture has been proven to be correct

- Just above the Erdős-Rényi curve [9].
- Just below the Erdős-Rényi curve when $e > 1/2$ [13].
- Near the line segment $e = 1/2$, $0 < t < 1/8$ [14].
- Just below the top boundary $t = e^{3/2}$ [18].
- Just above the bottom boundary when $e < 1/2$ [18].
- Just above each of the “scallops” on the lower right portion of the boundary, with the k -th scallop running from $e = \frac{k}{k+1}$ to $e = \frac{k+1}{k+2}$ [18].

That is, the optimal graphons in open subsets of the $F(1, 1)$, $B(1, 1)$, $A(2, 0)$, and $C(k, 2)$ phases, for every positive integer k , have been proven to exist, to be unique, and to have the form conjectured in [8].

However, there is also a region, with $e < e_0 := (3 - \sqrt{3})/6 \approx 0.2113$ and with t slightly below e^3 , where the optimal graphon is **not** described by the $A(2, 0)$ phase of Figure 2 [14]! Unfortunately, the proof that the typical structure is not $A(2, 0)$ did not provide any estimates for how big this exceptional region is or what the typical structure is. [14] exhibited a “tripodal” graphon that has more entropy than the “bipodal” $A(2, 0)$ graphon, but did not optimize the parameters of this tripodal graphon or rule out the possibility

that there is a different kind of graphon with even more entropy.

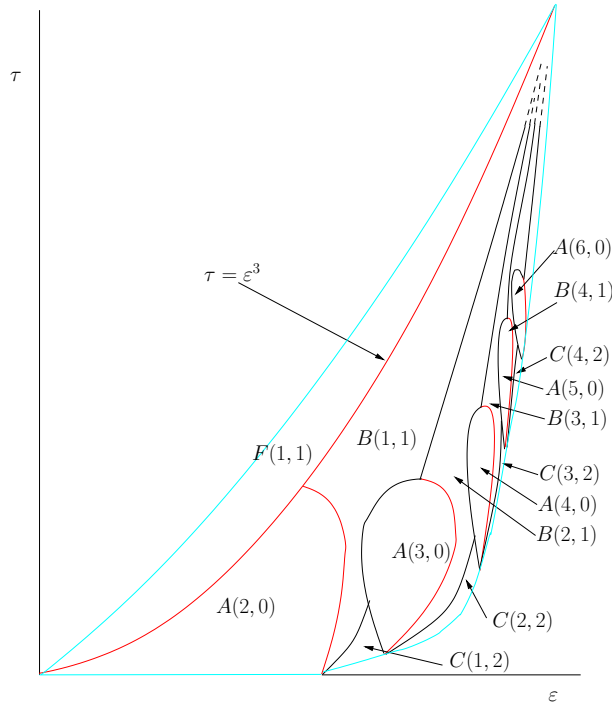


Fig. 2. A conjectured phase portrait in the edge/triangle model. The size and shape of each phase are only schematic. In a realistic rendering, many of the phases would be too small to see

In other words, Figure 2 needs to be amended, adding one or more mystery phases just below the Erdős-Rényi curve for $e < e_0$. In this paper we report on some numerical explorations of this *terra incognita*.

1.2. Multipodality and the ansatz of [14]

A graphon g is said to be k -podal if we can break the unit interval into k disjoint measurable regions I_1, \dots, I_k such that $g(x, y)$ is constant on each $I_i \times I_j$. A graphon that is k -podal for some k is said to be *multipodal* or a *step function*. The words “bipodal” and “tripodal” mean 2-podal and 3-podal, respectively. The regions I_i are called “podes”. After applying a measure-preserving transformation of $[0, 1]$, we can assume that each pode I_i is an interval and each $I_i \times I_j$ is a rectangle. A k -podal graphon g is then described by the sizes $|I_i|$ of the podes and by a symmetric $k \times k$ matrix giving the values of g on each rectangle.

An $(n + m)$ -podal graphon is said to have (n, m) *symmetry* if it is invariant under permutation of the first n podes and also invariant under permutation of the last m podes. In the conjectured phase diagram of Figure 2, all phases are multipodal with either $(n, 0)$, $(n, 1)$ or $(n, 2)$ symmetry, as indicated by the name of each phase. (In related models involving k -stars, all entropy maximizers have been proven to be multipodal [7]. However, proving multipodality for all phases in the edge/triangle model remains an open problem.)

The space of $(2, 0)$ -symmetric graphons is only 2-dimensional, so there is a unique graphon with edge/triangle densities (e, t) . This is shown in Figure 3, where $t = e^3 - \delta^3$.

The entropy of this “symmetric bipodal” graphon g_{sb} is

$$S(g_{sb}) = \frac{1}{2} \left(H(e + \delta) + H(e - \delta) \right) = H(e) + \frac{1}{2} H''(e) \delta^2 + O(\delta^4). \quad (4)$$

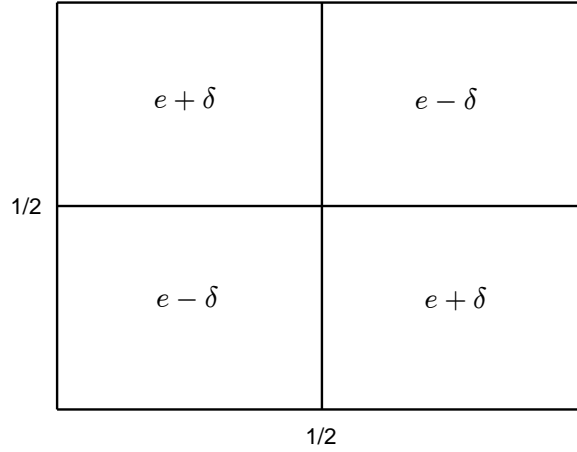


Fig. 3. The unique symmetric bipodal graphon with edge and triangle densities $(e, e^3 - \delta^3)$

Now consider the $(2, 1)$ -symmetric graphon of Figure 4, depending on parameters A , B , and c . Specifically, we have podes I_1 and I_2 , each of size $c/2$, and I_3 of size $1 - c$, and our graphon takes on the values

$$g(x, y) = \begin{cases} e - A + B(1 - c) & (x, y) \in (I_1 \times I_1) \cup (I_2 \times I_2), \\ e + A + B(1 - c) & (x, y) \in (I_1 \times I_2) \cup (I_2 \times I_1), \\ e - cB & (x, y) \in (I_1 \times I_3) \cup (I_2 \times I_3) \cup (I_3 \times I_1) \cup (I_3 \times I_2), \\ e + \frac{c^2}{1-c} B & (x, y) \in I_3 \times I_3. \end{cases} \quad (5)$$

The edge density is e and the triangle density is $e^3 - c^3(A^3 - B^3)$, so $c = \delta(A^3 - B^3)^{-1/3}$. Holding A and B fixed and considering the behavior as $c \rightarrow 0$, we have

$$\begin{aligned} S(g) &= \frac{c^2}{2} \left(H(e - A + B(1 - c)) + H(e + A + B(1 - c)) \right) \\ &\quad + 2c(1 - c)H(e - cB) + (1 - c)^2 H \left(e + \frac{c^2}{1 - c} B \right) \\ &= H(e) + \frac{1}{2} F(A, B) \delta^2 + O(\delta^3), \end{aligned} \quad (6)$$

where

$$F(A, B) = \frac{H(e + A + B) + H(e - A + B) - 2H(e) - 2BH'(e)}{(A^3 - B^3)^{2/3}}, \quad (7)$$

and we have used Taylor series to approximate $H(u)$ when $u \approx e$. If we can find parameters A and B such that $F(A, B) > H''(e)$, then for sufficiently small δ we have $S(g) > S(g_{sb})$. In [14], a power series expansion was used to show that such values of (A, B) exist, with A small and $B = O(A^2)$, whenever $e < e_0 := (3 - \sqrt{3})/6$.

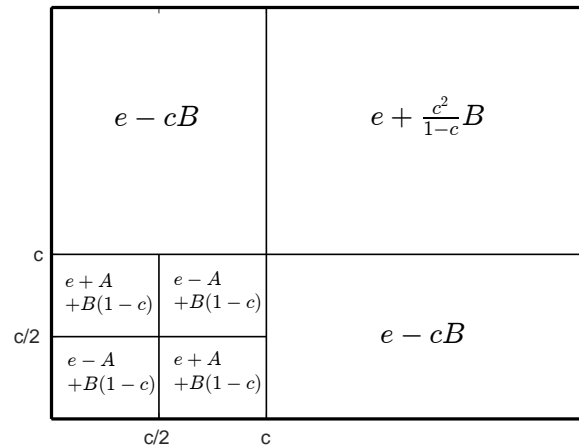


Fig. 4. A tripodal graphon with (2,1) symmetry and constant degrees

Remark 1.1. The expression (5) may look complicated and unintuitive. However, it is actually one of the simplest possible structures to improve on (4). By integrating a simple Taylor series expansion of $H(g(x, y))$ around $g(x, y) = e$ we obtain

$$S(g) = H(e) + \frac{1}{2}H''(e)\|g - e\|_{L^2}^2 + O(\|g - e\|_{L^2}^3) \leq H(e) + \frac{1}{2}H''(e)\delta^2 + o(\delta^2), \quad (8)$$

for all graphons g that are pointwise close to e . In order to obtain a coefficient of δ^2 that is greater than $\frac{1}{2}H''(e)$, we must consider instead a graphon that differs greatly from e on a subset of the unit square of measure $O(\delta^2)$.

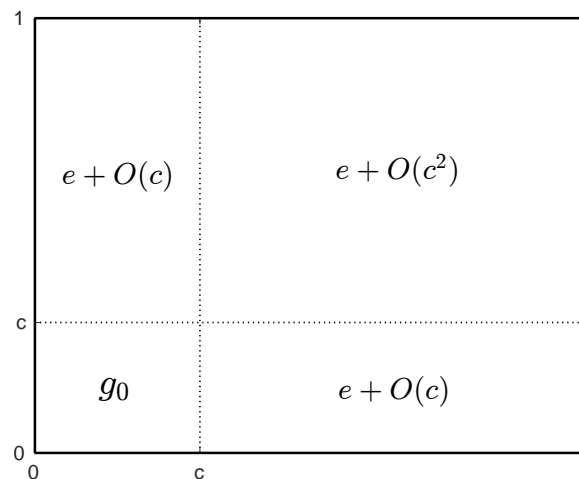


Fig. 5. A strategy for generating efficient graphons. The $O(c)$ and $O(c^2)$ terms are chosen to make the degree function exactly constant

This suggests the following general construction, see Figure 5. Start with an arbitrary graphon g_0 , with no constraints on the edge or triangle densities of g_0 . Let $I_1 = [0, c]$ for

some small constant c and let $I_2 = [c, 1]$. Let

$$g(x, y) = \begin{cases} g_0\left(\frac{x}{c}, \frac{y}{c}\right) & (x, y) \in I_1 \times I_1, \\ e - \frac{c}{1-c}d(x/c) & (x, y) \in I_1 \times I_2, \\ e - \frac{c}{1-c}d(y/c) & (x, y) \in I_2 \times I_1, \\ e + \frac{c^2}{(1-c)^2}B & (x, y) \in I_2 \times I_2. \end{cases} \quad (9)$$

where $d(x) = \int_0^1 g_0(x, y) dy$ is the degree function of g_0 and $B = \int_0^1 (d(x) - e) dx = \iint (g_0(x, y) - e) dx dy$ is the difference between the edge density of g_0 and e . That is, we put a rescaled copy of g_0 in the lower left corner of the unit square and adjust g on the rest of the square to keep the degree function constant, thereby minimizing $\|g - e\|_{L^2}$ for given δ and g_0 .

The triangle density for small c is easily computed in terms of g_0 :

$$\tau(g) = e^3 + c^3 \tau(g_0 - e) + O(c^4), \quad (10)$$

so

$$\delta = c \tau(e - g_0)^{1/3} + O(c^2). \quad (11)$$

We similarly compute the entropy of g to leading order in c , obtaining

$$\begin{aligned} S(g) &= c^2 S(g_0) + (1 - c^2)H(e) - c^2 B H'(e) + O(c^3) \\ &= H(e) + c^2 (S(g_0) - H(e) - B H'(e)) + O(c^3) \\ &= H(e) + \frac{\delta^2}{2} \left(\frac{2S(g_0) - 2H(e) - 2B H'(e)}{\tau(e - g_0)^{2/3}} \right) + O(\delta^3). \end{aligned} \quad (12)$$

The simplest version of this construction involves a constant graphon g_0 . That is *precisely* the asymptotic form of the optimal graphon when $e > 1/2$ and t is slightly less than e^3 [13].

The next simplest possibility is for g_0 to be symmetric bipodal. In that case, the general construction (9) reduces to (5), albeit with the constant B rescaled by a factor of $1 - c$. The coefficient of $\frac{\delta^2}{2}$ in (12) reduces to the function $F(A, B)$ of (7).

1.3. Organization of the paper

We extend the analysis of [14] with two goals in mind. First, we wish to find the actual entropy maximizing graphon g , not just a graphon that does better than g_{sb} . Second, we wish to explore the entire tripodal region, not just an infinitesimal neighborhood of the Erdős-Rényi curve.

(1) In Section 2 we determine the values of A and B that maximize $F(A, B)$, over a range of values of e . This is a problem in 2-variable calculus, not in functional analysis, and does not require any fancy methods. A combination of sampling on a grid and Newton's method is sufficient. As expected, it is possible to do better than $H''(e)$ precisely when $e < e_0$. We also discover a transition at $e \approx 0.0024$, where the best values of A and B change discontinuously.

(2) The set of possible graphons with (2,1) symmetry is slightly more general than the ansatz (5), with the degree function on the two poles differing in general by a quantity

$D/2$, with the original ansatz corresponding to $D = 0$. In Section 3 we explore (2,1)-symmetric graphons with D nonzero and show that the optimal value of D is $O(\delta^2)$, yielding an entropy that is $O(\delta^4)$ better than with $D = 0$. Since we are mostly looking at the entropy at order δ^2 , this $O(\delta^4)$ contribution does not change the overall picture. For a qualitative understanding of the tripodal phase and of phase transitions, the ansatz (5) is enough.

(3) In Section 4, we probe the size of the tripodal phase. Specifically, for each value of e we determine the range of δ values for which a (2,1)-symmetric tripodal graphon g has more entropy than a symmetric bipodal graphon. When δ reaches a certain size, the entropies of $S(g)$ and $S(g_{sb})$ become equal, indicating a phase transition. The graphon g does not become singular as we approach this point, nor does it approach g_{sb} . Instead, the optimal graphon changes discontinuously from g to g_{sb} .

We do this analysis twice, once for the ansatz and once allowing D to vary. There are small quantitative differences, but the entropies are close and the optimal values of (A, B) are nearly the same.

(4) Finally, in Section 5, we explore the transition near $e = 0.0024$. Assuming that the optimal graphon is either symmetric bipodal or (2,1)-symmetric tripodal, we determine the boundary between two distinct tripodal phases.

2. The maximum of $F(A, B)$

The ansatz (5) gives the most general graphon with (2,1) symmetry, with edge density e , and with constant degree function $d(x) = \int_0^1 g(x, y) dy$. Maximizing $F(A, B)$ is tantamount to maximizing the entropy among graphons with (2,1) symmetry and with triangle density just below e^3 .

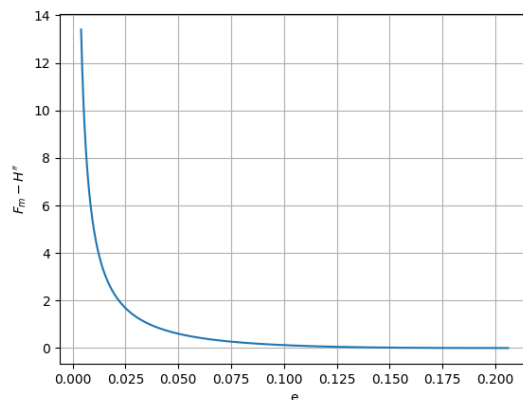


Fig. 6. $F_m(e) - H''(e)$ as a function of e

Let $F_m(e)$ be the maximum of $F(A, B)$ for a given edge density e . In order to compute $F_m(e)$, we first choose a value of e and plot $F(A, B)$ in Desmos two ways, once for each variable while leaving the other variable on a slider. By moving the sliders and looking at the corresponding cross sections of $F(A, B)$, we determine the approximate locations of the local maxima. We then apply Newton's method, starting at these approximate

locations, to localize the maximum to machine accuracy. Having done this for one value of e , we increment e in steps of 0.001 and use the optimal values of (A, B) from the previous e as the starting point for Newton's method for the new value of e . This process successfully evaluated the optimal values of A and B and the values of $F_m(e)$ for e between 0.033 and 0.206, see Figures 6 and 7. The same procedure, only with a smaller increment for e , allowed us to probe values of e that are smaller than 0.033 or larger than 0.206.

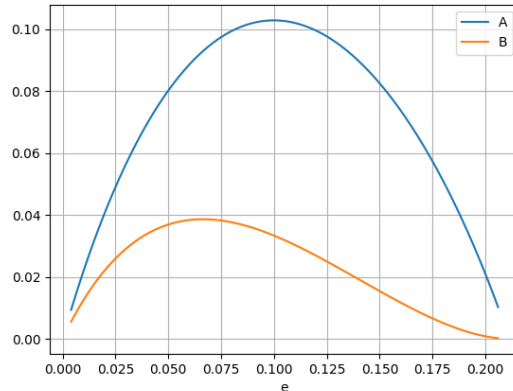


Fig. 7. The optimal values of A and B as functions of e

The relevant values of A and B go to zero as $e \rightarrow e_0$. To determine the rate of decay, we plot $\ln(A)$, $\ln(B)$ and $\ln(F_m - H'')$ versus $\ln(e_0 - e)$ in Figure 8. The plots are approximately linear as $e \rightarrow e_0$, with slopes 1, 2 and 3, respectively, indicating that $A \sim (e_0 - e)^1$, $B \sim (e_0 - e)^2$ and $F_m - H'' \sim (e_0 - e)^3$.

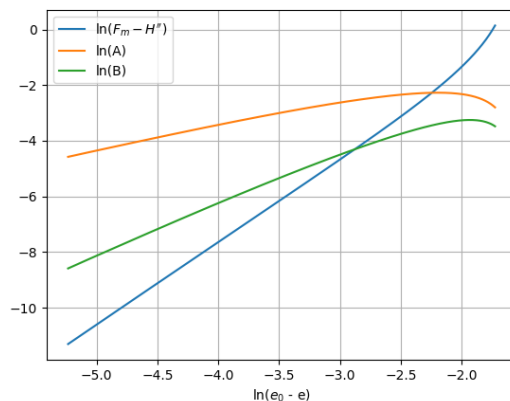


Fig. 8. The slopes of this log plot show how various functions scale with e as $e \rightarrow e_0$. A scales as $(e_0 - e)^1$, B as $(e_0 - e)^2$, and $F_m - H''$ as $(e_0 - e)^3$

Our procedure for maximizing $F(A, B)$ is guaranteed to find a *local* maximum near the previous best values of (A, B) . To ensure that we are not missing a separate (and potentially higher) local maximum, we re-examined the function $F(A, B)$ on Desmos by eye for selected values of e . This turned out to be unnecessary for $e > 0.01$, where the

local maximum found by our iterated Newton's method procedure is indeed the global maximum. However, things are different when e is very small.

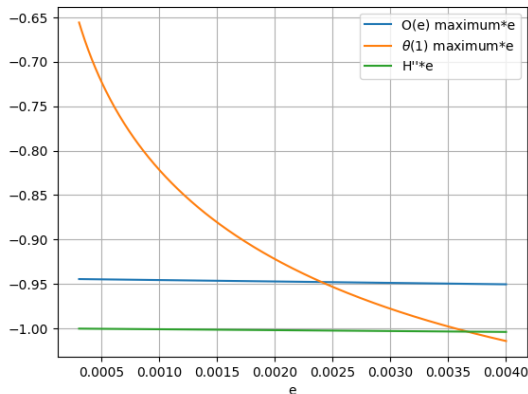


Fig. 9. The two local maxima of $F(A, B)$ for small e , compared to $H''(e)$

This is seen in Figure 9. There are two local maxima in the $F(A, B)$ plot. One, with $A \approx 2.5e$ and $B \approx 1.5e$, yields values of $F(A, B)$ that are a few percent better than $H''(e)$, being close to $-0.95/e$ while $H''(e) \approx -1/e$. The other, with A and B close to $1/2$, dominates when $e < 0.0024$. To get an algebraic understanding of this numerical result, consider $F(A, B)$ when $A = \frac{1}{2}$ and $B = \frac{1}{2} - e$. (These particular values, while not optimal, give a lower bound for $F_m(e)$ and an upper bound for $F_m(e)/H''(e)$.) In that case,

$$\begin{aligned} F(A, B) &= \frac{H(e + A + B) + H(e - A + B) - 2H(e) - 2BH'(e)}{(A^3 - B^3)^{2/3}} \\ &= \frac{-2H(e) - (1 - 2e)H'(e)}{\left(\frac{3}{4}e - \frac{3}{2}e^2 + e^3\right)^{2/3}}, \end{aligned} \quad (13)$$

since $H(e + A + B) = H(1) = 0$ and $H(e - A + B) = H(0) = 0$. As $e \rightarrow 0$, the numerator scales as $\ln(e)$, while the denominator scales as $e^{2/3}$, so $F(A, B)$ scales as $e^{-2/3} \ln(e)$. Since $H''(e) = -\left(\frac{1}{e} + \frac{1}{1-e}\right)$ scales as e^{-1} , the ratio $F_m(e)/H''(e)$ goes to zero at least as fast as $e^{1/3} \ln(e)$.

The switch from one local maximum to another at $e \approx 0.0024$ indicates that there must be at least one phase transition when e is small, in addition to the transition between tripodal and bipodal graphons. However, it does not tell us what the phase transition looks like.

The simplest possibility is that there are two (2,1)-symmetric phases, with the boundary between them hitting the Erdős-Rényi curve at $e \approx 0.0024$. Recall that maximizing $F(A, B)$ is tantamount to determining the best (2,1)-symmetric graphon for t slightly less than e^3 . When $e \gtrsim 0.0024$ and t is slightly less than e^3 , the optimal graphon is (2,1)-symmetric tripodal with all values on the order of e , in particular with all values less than 0.01. When $e \lesssim 0.0024$ and t is slightly less than e^3 , the optimal graphon takes values close to 1 on $I_1 \times I_2$. On the curve separating the two phases, the optimal graphon changes discontinuously. We will consider this possibility further in Section 5.

However, it's also possible that analyzing the best (2,1)-symmetric tripodal graphon for very small values of e is moot. Maybe the best graphons are tripodal with no symmetry at all, or 4-podal, or 5-podal, and so on. Our data does not rule this out, nor does it rule out an infinite cascade of phases as we approach $(e, t) = (0, 0)$, just as there are infinitely many phases with $(n, 0)$ or $(n, 1)$ or $(n, 2)$ symmetry as we approach $(e, t) = (1, 1)$. Exploring these possibilities is a problem for future research.

Remark 2.1. Finding the best graphon for t close to e^3 is closely connected to the problem of moderate deviations. Graphs with n vertices and a fixed density e of edges have an expected density of triangles that is close to e^3 and a standard deviation that scales as $n^{-3/2}$. Fluctuations in the triangle density of order $n^{-3/2}$ are called *small deviations* and are governed by the central limit theorem. Fluctuations of order 1 are called *large deviations* and are governed by graphons that maximize $S(g)$ subject to constraints on $\varepsilon(g)$ and $\tau(g)$. Fluctuations of order n^α , where $-3/2 < \alpha < 0$, are called *moderate deviations* and are more complicated.

When $e > 1/2$, moderate deviations with $\alpha > -1$ and with fewer triangles than expected (“undersaturated graphs” or “lower tails”) turn out to be governed by the same graphons that describe the $t \rightarrow e^3$ limit of large deviations [1, 12], while those with $\alpha < -1$ are qualitatively similar to small deviations [5]. However, understanding moderate deviations with $e < 1/2$ is complicated by the fact that we don't know what the optimal graphons are for large deviations. That's what we're trying to figure out in this paper! It appears likely that the limiting form of the optimal graphons as $\delta \rightarrow 0$ will shed light on moderate deviations.

In particular, we can study moderate deviations in the limit as $e \rightarrow 0$. When considering upper tails of triangle counts in sparse graphs, the structure derived by [6] can be viewed as an $e \rightarrow 0$ limit of the graphons found in [9]. While we do not know what the best graphon actually is, the ansatz (5) with $A = \frac{1}{2}$ and $B = \frac{1}{2} - e$ gives a lower bound on the entropy that is much higher than anything previously known. This suggests a technique for studying moderate deviations for undersaturated sparse graphs.

3. Moving beyond the ansatz

We now consider arbitrary tripodal graphons with (2,1)-symmetry. To describe such graphons, we need some notation. Let g_{ij} be the value of a graphon on $I_i \times I_j$ and let c_i be the width of the i -th pole. Because of our (2,1)-symmetry, we have $c_1 = c_2$, $g_{11} = g_{22}$ and $g_{13} = g_{23}$. The entire graphon can be expressed in terms of four parameters A , B , c , and D , with

$$\begin{aligned} c_1 &= c_2 = c/2, \\ c_3 &= 1 - c, \\ g_{11} &= g_{22} = e - A + (1 - c)(B + D), \\ g_{12} &= e + A + (1 - c)(B + D), \\ g_{13} &= g_{23} = e - cB + \frac{1 - 2c}{2}D, \end{aligned}$$

$$g_{33} = e + \frac{c^2}{1-c}B - cD. \quad (14)$$

When $D = 0$, this reduces to the ansatz (5). The extra terms account for changes in the degree function from one node to another. The degree function is then

$$d(x) = \begin{cases} e + \frac{1-c}{2}D, & x < c, \\ e - \frac{c}{2}D, & x > c. \end{cases} \quad (15)$$

This graphon can be described more succinctly in terms of the functions

$$v_1(x) = \begin{cases} 1, & x < c/2, \\ -1, & c/2 < x < c, \\ 0, & x > c, \end{cases} \quad v_2(x) = \begin{cases} \sqrt{1-c}, & x < c, \\ \frac{-c}{\sqrt{1-c}}, & x > c. \end{cases} \quad (16)$$

These functions are orthogonal in $L^2([0, 1])$, with $\|v_1\|_{L^2}^2 = \|v_2\|_{L^2}^2 = c$. Our graphon is then

$$g(x, y) = e - Av_1(x)v_1(y) + Bv_2(x)v_2(y) + \frac{D}{2}\sqrt{1-c}(v_2(x) + v_2(y)). \quad (17)$$

Since the functions v_1 and v_2 integrate to zero, our edge density is exactly e . Defining $\delta g(x, y) = g(x, y) - e$, the triangle density is easily computed from the expansion

$$\begin{aligned} \tau(g) &= e^3 + 3e \int_0^1 (d(x) - e)^2 dx + \tau(\delta g) \\ &= e^3 + \frac{3}{4}ec(1-c)D^2 + \frac{3}{4}c^2(1-c)BD^2 + c^3(B^3 - A^3). \end{aligned} \quad (18)$$

Finally, the entropy is

$$\begin{aligned} S &= \frac{c^2}{2} \left(H(e - A + (1-c)(B + D)) + H(e + A + (1-c)(B + D)) \right) \\ &\quad + 2c(1-c)H \left(e - cB + \frac{1-2c}{2}D \right) + (1-c)^2 H \left(e + \frac{c^2}{1-c}B - cD \right). \end{aligned} \quad (19)$$

We also compute the first two derivatives of S with respect to D at $D = 0$:

$$\begin{aligned} \frac{\partial S}{\partial D} &= \frac{1}{2}c^2(1-c)(H'(e - A + B(1-c)) + H'(e + A + B(1-c))) \\ &\quad + c(1-c)(1-2c)H'(e - cB) - c(1-c)^2 H' \left(e + \frac{c^2}{1-c}B \right) \\ &\approx \frac{c^2(1-c)}{2} (H'(e - A + B(1-c)) + H'(e + A + B(1-c)) - 2H'(e) - 2B(1-c)H''(e)), \\ \frac{\partial^2 S}{\partial D^2} &= \frac{c^2(1-c)^2}{2} (H''(e - A + B(1-c)) + H''(e + A + B(1-c))) \\ &\quad + \frac{c(1-c)(1-2c)^2}{2} H''(e - cB) + c^2(1-c)^2 H'' \left(e + \frac{c^2}{1-c}B \right) \\ &= \frac{c}{2}H''(e) + O(c^2), \end{aligned} \quad (20)$$

where in estimating $\partial S/\partial D$ we have used the linear approximations $H'(e - cB) \approx H'(e) - cBH''(e)$ and $H'(e + \frac{c^2}{1-c}B) \approx H'(e) + \frac{c^2}{1-c}BH''(e)$.

Having D nonzero can increase the entropy by $O(\delta^2 D)$, but at a cost of increasing the triangle density by $\frac{3}{4}c(1-c)(e+Bc)D^2$. These must be compensated with other changes to the graphon. Since $\partial S/\partial t$ scales as δ^{-1} , and since c scales as δ^1 , there is effectively a $\Theta(D^2)$ entropy cost for having $D \neq 0$, in addition to the $O(cD^2)$ cost from $\partial^2 S/\partial D^2$. Balancing the cost and benefit, the optimal value of D is $O(\delta^2)$, with the result that the D terms only contribute to the entropy at order δ^4 .

We conclude that the difference between the ansatz graphon (5) and the most general (2,1)-symmetric graphon (14) is small, especially close to the Erdős-Rényi curve. It has a non-negligible effect on establishing the boundary between the tripodal phase and the symmetric bipodal phase, but does not change the qualitative picture. When it comes to a qualitative understanding of the tripodal phase, it is sufficient to work with the ansatz (5).

4. The extent of the tripodal phase

So far, we have only considered graphons with t infinitesimally close to e^3 . That is, setting $t = e^3 - \delta^3$, we have been looking at the $\delta \rightarrow 0$ limit. In this section we consider how big δ can get and still have a (2,1)-symmetric tripodal graphon with more entropy than the symmetric bipodal graphon. In other words, we want to understand how far down the (2,1)-symmetric tripodal phase extends in the (e, t) plane. We also examine the nature of the phase transition from tripodal to symmetric bipodal.

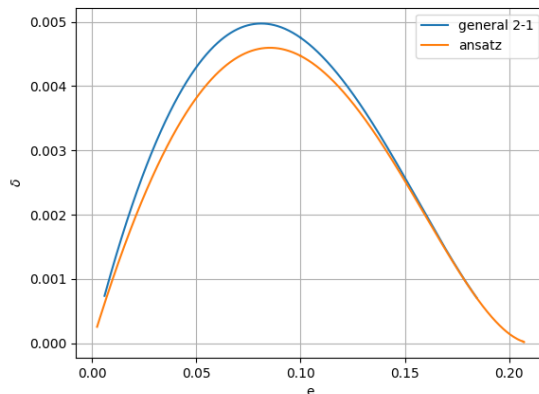


Fig. 10. The maximum value of δ for which the ansatz (5) or the most general (2,1)-symmetric graphon has more entropy than a symmetric bipodal graphon

4.1. Results

The maximum value of δ is shown in Figure 10, both allowing $D \neq 0$ (the blue curve) and restricting our attention to $D = 0$ (the orange curve). Note that

- The largest possible values of δ in the tripodal phase occur at $e \approx 0.08$. Both as $e \rightarrow e_0$ and as $e \rightarrow 0$, the maximum value of δ goes to zero.
- When $e > 0.0024$, δ is never greater than $0.11e$. Since $t = e^3 - \delta^3$, this means that

tripodal phase is almost completely contained in the region $0.998e^3 < t < e^3$. In terms of the variables (e, t) , the tripodal phase is extremely small and very easy to miss.

- The blue and orange curves are qualitatively similar, but have noticeable differences when $e < 0.12$ or so.

- We have calculated the orange curve for essentially the entire interval $[0.0024, e_0]$. However, calculating the blue curve is numerically less stable, so we only have results for $e > 0.01$. We will discuss the small e regime further in Section 5.

We next consider how the optimal graphon evolves as we traverse the phase by increasing δ , starting at $\delta = 0$. For $e = 0.1$, this is shown in Figure 11. The boundary of the phase at $\delta \approx 0.0048$ is not characterized by any dramatic behavior. It is simply the point where the optimal (2,1)-symmetric graphon happens to have the same entropy as a symmetric bipodal graphon, meaning that the constrained optimization problem does not have a unique solution. To the left of the dotted line, the data indicate that the optimal graphon is (2,1)-symmetric with the parameter values shown in the figure. To the right of the dotted line, the figure only shows a local maximum of the entropy, with the actual optimal graphon being symmetric bipodal.

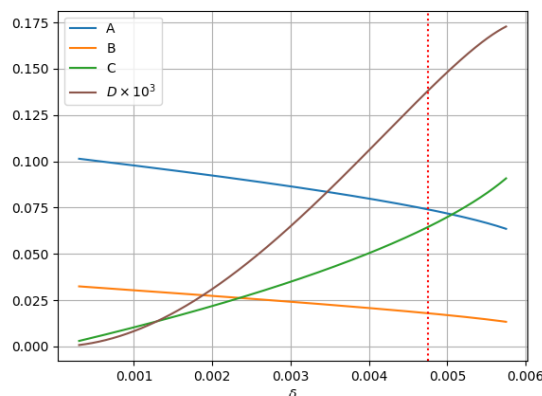


Fig. 11. For a fixed value of $e = 0.1$, the optimal values of A, B, c, D as functions of δ , scaled to fit in the same plot. The dotted line shows where the optimal graphon is overtaken in entropy by a symmetric bipodal graphon

The picture is similar for other values of e , see Figure 12. As δ increases from zero, c increases linearly and D increases, first quadratically and then roughly linearly, while A and B gradually decrease. The phase transition does not correspond to any singularities in the parameters (A, B, c, D) . Rather, it is a point where we jump discontinuously from a graphon described by these parameters to a symmetric bipodal graphon. The relative size of D versus A, B and c is different for different values of e , but the graphs of (A, B, c) are all qualitatively the same.

Finally, we compare the optimal (2,1)-symmetric graphon to the ansatz (5). Figure 13 shows the situation when $e = 0.1$, with the optimal values of (A, B, c) for general D (in solid lines) compared to the optimal values for $D = 0$ (in dotted lines). The differences are minor. Allowing $D \neq 0$ does yield greater numerical accuracy, but it doesn't change the overall story.

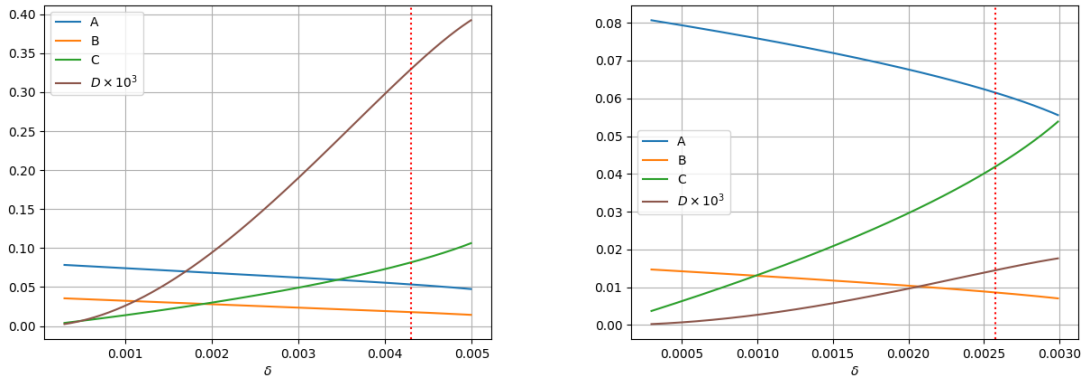


Fig. 12. The dependence of (A, B, c, D) on δ for $e = 0.05$ and $e = 0.15$

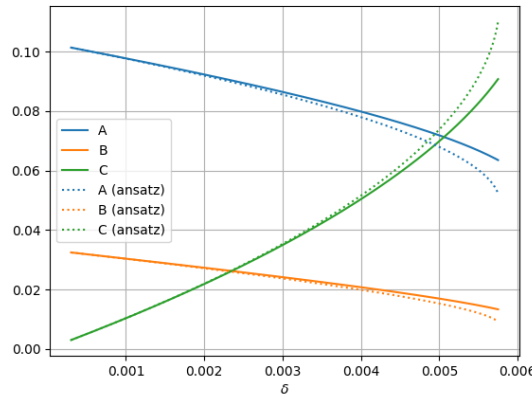


Fig. 13. When $e = 0.1$, the optimal values of (A, B, c) for $D = 0$ (dotted lines) are nearly identical to those where we allow $D \neq 0$

4.2. *Methods*

In generating Figure 10, we sought the value of δ for which the entropy of the best possible (2,1)-symmetric graphon equals the entropy of a symmetric bipodal graphon. We found this value of δ , which we call δ_m , in three steps. We first determined δ_m to within 0.0001 for $e = 0.1$. Next we used Newton’s method to home in on the true value of δ_m for $e = 0.1$. Finally, we varied e and used Newton’s method to track the changes in δ_m as a function of e . We did this 3-step process twice, once assuming $D = 0$ (that is, the ansatz (5)) and once allowing D to float.

We now describe the three steps for the ansatz and then note the differences for $D \neq 0$.

(1) We began at $(e, \delta) = (0.1, 0)$ and chose A and B to maximize $F(A, B)$, as in Section 2. We then incremented δ in steps of 0.0001. At each new value of δ , we solved for c in terms of (A, B) and wrote the entropy as a function of (A, B) . We maximized that entropy, using the optimal values of (A, B) from the previous value of δ as the starting point for Newton’s method. We recorded the resulting entropy and compared it to that of a symmetric bipodal graphon, continuing until the tripodal entropy dropped below the symmetric bipodal entropy. The true value of δ_m then lay between the last two values of

δ .

(2) Once we knew δ_m to within 0.0001 and knew the corresponding values of (A, B) , we alternated between two forms of Newton's method to obtain more accuracy. First we held (A, B) fixed and varied δ to equate the entropy of our tripodal graphon with the entropy of a symmetric bipodal graphon. Then we held δ fixed and varied (A, B) to maximize the entropy for the given δ . We alternated between these two calculations, converging to a triple (A, B, δ) that maximized entropy for the given δ and that had the same entropy as a symmetric bipodal graphon. This gave us δ_m for $e = 0.1$ to machine accuracy.

(3) For other values of e , we did not start at $\delta = 0$. Instead, we incremented (or decremented) e in steps of 0.001, using the values of (A, B, δ_m) from the previous value of e as the starting point for an alternating pair of Newton's method calculations, as in Step 2. This filled out the rest of the orange curve in Figure 10.

The calculations for $D \neq 0$ were similar, only with a few adjustments. Since the optimal D is $O(\delta^2)$, we started at $(e, \delta) = (0.1, 0)$, with the same values of (A, B) as before and with $D = 0$. For each new δ , we eliminated A rather than c and used Newton's method to obtain values of (B, c, D) that maximized the entropy. In the second and third steps, we alternated between varying δ while holding (B, c, D) fixed (to equate the tripodal and bipodal entropies) and varying (B, c, D) with δ fixed (to maximize the tripodal entropy). These calculations generated the blue curve.

To generate Figures 11–13, we repeated the first step of the above calculation. That is, we started at $(e, \delta) = (0.1, 0)$ or $(0.05, 0)$ or $(0.15, 0)$, with $D = 0$ and with (A, B) maximizing $F(A, B)$. We gradually increased δ , eliminated one variable (c or A), and used several rounds of Newton's method on the remaining variables to maximize the entropy, using data from the previous value of δ as a starting point. This gave (A, B, c) or (A, B, c, D) as functions of δ .

5. Graphs with low edge density

We now examine graphons whose edge density is close to zero. As we saw in Section 2, there are two local maximizers of $F(A, B)$, one with $A \approx 2.5e$ and $B \approx 1.5e$ and the other with $A \approx \frac{1}{2}$ and $B \approx \frac{1}{2} - e$. As δ increases, this gives rise to two families of (2,1)-symmetric tripodal graphons, each of which is a local entropy maximizer in the space of (2,1)-symmetric graphons. Based on the size of A and B , we refer to the first as the “ $O(e)$ solution” and the second as the “ $\Theta(1)$ solution”.

In Section 4 we compared the entropy of the $O(e)$ solution to the entropy of a symmetric bipodal graphon and determined the largest value of δ for which the first was greater than the second. Here we compare the entropies of the $O(e)$ and $\Theta(1)$ solutions to each other and to that of a symmetric bipodal graphon, using essentially the same numerical methods as in Section 4.

The results are summarized as follows:

- When $e > 0.0024$ or so, the $\Theta(1)$ solution never does better than the $O(e)$ solution. The entire tripodal region takes the $O(e)$ form and extends from Erdős-Rényi to the value of δ given by the orange curve of Figure 14 or the blue curve of Figure 10. This is the

phase that we previously studied in Section 4.

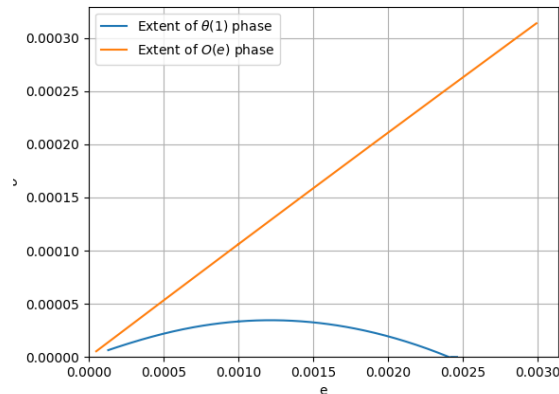


Fig. 14. As a function of e , the values of δ at which the $\Theta(1)$ phase transitions to $O(e)$ (blue) and at which the $O(e)$ phase transitions to symmetric bipodal (orange)

- When $e < 0.0024$, $F(A, B)$ is maximized with $(A, B) = \Theta(1)$, so the optimal graphon for sufficiently small values of δ takes the $\Theta(1)$ form. However, the $O(e)$ solution does better for larger values of δ , outperforming both $\Theta(1)$ and symmetric bipodal. See Figure 14 for the values of δ where we transition from $\Theta(1)$ to $O(e)$, and where we then transition from $O(e)$ to symmetric bipodal.

- Considering all values of e , the tripodal region consists of two distinct phases. The $\Theta(1)$ phase hugs the Erdős-Rényi curve very tightly for $e < 0.0024$ and is separated from the symmetric bipodal phase by the $O(e)$ phase. This phase is similar in shape to the $O(e)$ phase, which hugs the ER curve for $e < e_0 \approx 0.2113$. However, the $\Theta(1)$ phase is *much* smaller, being limited to $e < 0.0024$ and roughly $0.9999e^3 < t < e^3$.

- When speaking of the $O(e)$ and $\Theta(1)$ phases, we have implicitly assumed that the optimal graphon is either bipodal or (2,1)-symmetric tripodal. It is possible that part of what we call the $O(e)$ phase, and part or all of the $\Theta(1)$ phase, is actually in an asymmetric tripodal phase or a more complicated multipodal phase. We have seen no evidence to suggest such complicated structures, but at this point we cannot rule them out.

Acknowledgments

We thank Charles Radin for helpful discussions. This work is partially supported by the National Science Foundation. For access to our numerical data, please contact the first author.

References

- [1] J. Alvarado, G. Dias, and S. Griffiths. Moderate deviations of triangle counts in the Erdős-Rényi random graph: the lower tail. arXiv:2403.13792, 2024. <https://arxiv.org/abs/2403.13792>.

-
- [2] C. Borgs, J. Chayes, and L. Lovász. Moments of two-variable functions and the uniqueness of graph limits. *Geometric and Functional Analysis*, 19:1597–1619, 2010. <https://doi.org/10.1007/s00039-010-0044-0>.
- [3] C. Borgs, J. Chayes, L. Lovász, V. Sós, and K. Vesztegombi. Convergent graph sequences i: subgraph frequencies, metric properties, and testing. *Advances in Mathematics*, 219(6):1801–1851, 2008. <https://doi.org/10.1016/j.aim.2008.07.008>.
- [4] S. Chatterjee and S. R. S. Varadhan. The large deviation principle for the Erdős–Rényi random graph. *European Journal of Combinatorics*, 32(7):1000–1017, 2011. <https://doi.org/10.1016/j.ejc.2011.03.014>.
- [5] C. Goldschmidt, S. Griffiths, and A. Scott. Moderate deviations of subgraph counts in the Erdős–Rényi random graphs $G(n, m)$ and $G(n, p)$. *Transactions of the American Mathematical Society*, 373:5517–5585, 2020. <https://doi.org/10.1016/j.ejc.2025.104189>.
- [6] M. Harel, F. Mousset, and W. Samotij. Upper tails via high moments and entropic stability. *Duke Mathematical Journal*, 171(10):2089–2192, 2022. <https://doi.org/10.1215/00127094-2021-0067>.
- [7] R. Kenyon, C. Radin, K. Ren, and L. Sadun. Multipodal structures and phase transitions in large constrained graphs. *Journal of Statistical Physics*, 168:233–258, 2017. <https://doi.org/10.1007/s10955-017-1804-0>.
- [8] R. Kenyon, C. Radin, K. Ren, and L. Sadun. The phases of large networks with edge and triangle constraints. *Journal of Physics A*, 50:435001, 2017. <https://doi.org/10.1088/1751-8121/aa8ce1>.
- [9] R. Kenyon, C. Radin, K. Ren, and L. Sadun. Bipodal structure in oversaturated random graphs. *International Mathematics Research Notices*, 2018(4):1009–1044, 2018. <https://doi.org/10.1093/imrn/rnw261>.
- [10] L. Lovász. *Large Networks and Graph Limits*. American Mathematical Society, Providence, 2012.
- [11] L. Lovász and B. Szegedy. Limits of dense graph sequences. *Journal of Combinatorial Theory, Series B*, 96(6):933–957, 2008. <https://doi.org/10.1016/j.jctb.2006.05.002>.
- [12] J. Neeman, C. Radin, and L. Sadun. Moderate deviations in cycle count. *Random Structures & Algorithms*, 63(3):779–820, 2023. <https://doi.org/10.1002/rsa.21147>.
- [13] J. Neeman, C. Radin, and L. Sadun. Typical large graphs with given edge and triangle densities. *Probability Theory and Related Fields*, 168:1167–1223, 2023. <https://doi.org/10.1007/s00440-023-01187-8>.
- [14] J. Neeman, C. Radin, and L. Sadun. Existence of a symmetric bipodal phase in the edge-triangle model. *Journal of Physics A*, 57:095003, 2024. <https://doi.org/10.1088/1751-8121/ad259d>.
- [15] O. Pikhurko and A. Razborov. Asymptotic structure of graphs with the minimum number of triangles. *Combinatorics, Probability and Computing*, 26(1):138–160, 2017. <https://doi.org/10.1017/S0963548316000110>.
- [16] C. Radin and L. Sadun. Phase transitions in a complex network. *Journal of Physics A*, 46:305002, 2013. <https://doi.org/10.1088/1751-8113/46/30/305002>.

-
- [17] C. Radin and L. Sadun. Optimal graphons in the edge-2star model. arXiv:2305.00333, 2023. <https://arxiv.org/abs/2305.00333>.
- [18] C. Radin and L. Sadun. Emergence in graphs with near-extreme constraints. arXiv:2411.14556, 2024. <https://arxiv.org/abs/2411.14556>.
- [19] A. Razborov. On the minimal density of triangles in graphs. *Combinatorics, Probability and Computing*, 17(4):603–618, 2008. <https://doi.org/10.1017/S0963548308009085>.
- [20] D. Strauss. On a general class of models for interaction. *SIAM Review*, 28:513–527, 1986. <https://doi.org/10.1137/1028156>.

William DiCarlo

Department of Mathematics, University of Texas, Austin, Texas USA

E-mail will.a.dicarlo@utmail.utexas.edu

Lorenzo Sadun

Department of Mathematics, University of Texas, Austin, Texas USA

E-mail sadun@math.utexas.edu